JOURNAL OF MATERIALS SCIENCE 30 (1995) 133–141

Effect of Cr_2O_3 on the electrical properties of multicomponent ZnO varistors at the pre-breakdown region

S. A. PIANARO
Departamento de Engenharia de Materiais, Universidade Estadual de Ponta Grossa, Caixa Postal: 663, 84031510 Ponta Grossa, Pr Brazil

E. C. PEREIRA, L. O. S. BULHÕES, E. LONGO*
LIEC-DQ, Universidade Federal de São Carlos, Caixa Postal: 676, 13565-905 São Carlos, SP Brazil

J. A. VARELA
Instituto de Química, UNESP, Caixa Postal: 355, 14800900 Araraquara, SP Brazil

The effect of Cr_2O_3 on the electrical properties of the multicomponent ZnO varistors was investigated using voltage–current curves and impedance spectroscopy. The structure and morphological modifications were analysed by X-ray diffraction and scanning electron microscopy, respectively. It was observed in samples with addition 0.1 mol% Cr_2O_3 that there was an improvement in the electrical properties of the varistors, but the increase in concentration had a deleterious effect on the potential barrier at the grain boundary. The excess Cr_2O_3 segregates at the grain-boundary region and increases the donor concentration, leading to a higher leakage current.

1. Introduction

Zinc oxide varistors are ceramic devices with high non-linearity in their current–voltage behaviour [1]. Moreover, these materials show high-energy absorption capacity, low residual voltage, small leakage current and fast response to voltage transients [2–4]. These properties allow the application of these materials as protecting devices against voltage transients in electronic and industrial equipments and as surge arrestors [2–6].

The chemical compositions of traditional varistors [1] consist of minor additions of several metal oxides, such as Bi_2O_3, Sb_2O_3, CoO, MnO_2 and Cr_2O_3, to the ZnO powder. During the sintering process, these oxides react with ZnO leading different phases [7–11].

The non-ohmic properties of ZnO varistors are associated with the high resistivity of the grain-boundary region [12]. A grain-boundary defect model was proposed in the literature [13, 14] which is associated with a double Schottky barrier. In this model, trivalent substitutional ions ($Bi^{\bullet}$, $Sb^{\bullet}$, etc.), oxygen vacancies ($V_O^{\bullet}$, $V_O^{\bullet\bullet}$) and interstitials zinc ($Zn_i^{\bullet}$, $Zn0_i^{\bullet\bullet}$) positively charged, extend from both sides of the grain boundary of two adjacent grains. These charges are compensated by a layer of negative zinc ion vacancies (V'_{Zn} and V''_{Zn}) at the grain-boundary interface in order to maintain the electrical neutrality. Recently, it has been shown that O'_{ads} has an important role in the barrier formation [15]. Thus, a potential barrier is created which depends on the nature and concentration of the intrinsic and extrinsic defects localized at the grain boundary. The dopants are used to control the grain-boundary properties in order to obtain a higher barrier and narrower depletion layer. In the literature, there are many papers about the influence of the CoO and MnO_2 on the electrical behaviour of ZnO varistors [16–20]. However, little attention has been given to the Cr_2O_3 influence. In this paper we describe the effect of Cr_2O_3 on the electrical behaviour and morphology of a ZnO multicomponent varistor.

2. Experimental procedure

The conventional oxide mixing process was used to fabricate the samples. The purity and origin of the oxide were as follows: ZnO (99.9%, Uniroyal); Bi_2O_3 (99.0%, Riedel); Sb_2O_3 (99.1%, Baker); CoO (99.0%, Riedel); MnO_2 (90%–95%, Riedel) and Cr_2O_3 (99.0% Vetec). The samples were prepared with the following chemical compositions: $(95.0 - x)\%$ ZnO + 0.5% Bi_2O_3 + 1.5%Sb_2O_3 + 1.5% CoO + 1.5% MnO_2 + $x\%$ Cr_2O_3 (mol%), with x ranging from 0.0–0.8 mol%. In order to simplify the notation, the varistor system will be called ZBSCMCr.

The oxides were mixed and pressed isostatically under 210 MPa. The sintering was performed in air at

* Author to whom all correspondence should be addressed.

0022–2461

1250 °C for 1 h with a cooling rate of 180 °C h^{-1} in a Lindberg type box furnace. The samples were ground with a 400 mesh silicon carbide abrasive paper until the thickness of the pellets reached 1.0 mm. Silver electrodes were painted on both surfaces of the pellet followed by thermal treatment at 500 °C for 15 min.

The current–voltage experiments were performed using a low current range with a stabilized voltage source Tectrol TCY 600 at 25 °C. The α coefficients were calculated with a minimum square linear regression method from the log$J$–log$E$ curve in the range 1–10 mA cm^{-2}. The impedance spectroscopy measurements were conducted at different temperatures between 200 and 550 °C with a Solartron frequency response analyser model 1260, using a 2.0 V a.c. signal in the frequency range from 1 Hz up to 10 MHz.

The microstructural characterizations were performed with fractured surfaces of the samples which were polished and attacked with a 6 N NaOH solution for 1 min for microstructure revelation. These analyses were realized with an EDS probe attached to a Jeol microscope. The ceramic phases were characterized by X-ray diffraction. In order to obtain larger amounts of secondary phases, the ZnO matrix was solubilized with a 20% $HClO_4$–ethanol solution for 72 h as suggested by Santhanam *et al.* [8]. The precipitated obtained was filtrated, washed with an $HClO_4$–ethanol solution, dried and characterized.

3. Results and discussion

The electric field, E, versus current density, J, curves of the systems ZBSCMCr with Cr_2O_3 in the range from 0.0–0.8 mol% are shown in Fig. 1. The sample with 0.1 mol% Cr_2O_3 exhibits a better non-linear characteristic with a higher non-linear coefficient. However, samples with Cr_2O_3 concentrations higher than 0.1 mol% show a deleterious behaviour on the electric properties, because the α values were lowered, as shown in Table I. The breakdown voltages that depend on the grain size were measured at 1 mA cm^{-2} and practically do not change with the increase of the Cr_2O_3 concentration from 0.1–0.8 mol% (Table I).

TABLE I Breakdown voltage and α coefficients for the system ZBSCMCr with different Cr_2O_3 concentrations

Cr_2O_3 (mol %)	α	E_R (V cm^{-1})
0.0	34.7	2811
0.1	40.3	2491
0.5	32.8	2622
0.8	20.8	2500

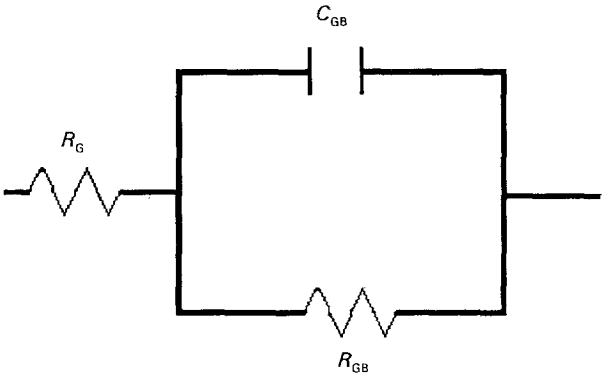

Figure 2 Equivalent circuit for a ZnO varistor.

The electronic transport in the varistors is normally associated with an RC equivalent circuit [12] shown in Fig. 2. The symbols in Fig. 2 denote the grain resistance, R_G, grain-boundary resistance, R_{GB}, and grain-boundary capacitance, C_{GB}. The a.c. electrical data were analysed using the Cole–Cole and Bode plots. From the analysis of these diagrams, we propose the existence of one time constant in the varistor associated with the electronic transport. Fig. 3 shows the Cole–Cole diagrams for the ZBSCMCr varistor

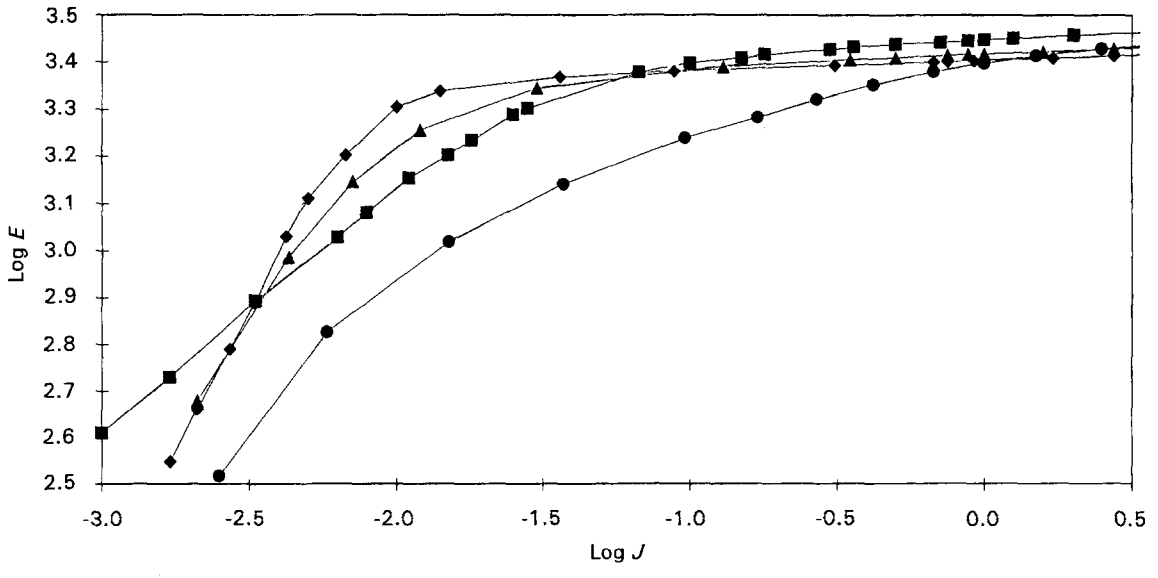

Figure 1 Electric field as function of current density curves for ZBSCMCr system with Cr_2O_3 concentration between 0.0 and 0.8 mol %. (■) 0.0% Cr_2O_3, (◆) 0.1% Cr_2O_3, (▲) 0.5% Cr_2O_3, (●) 0.8% Cr_2O_3.

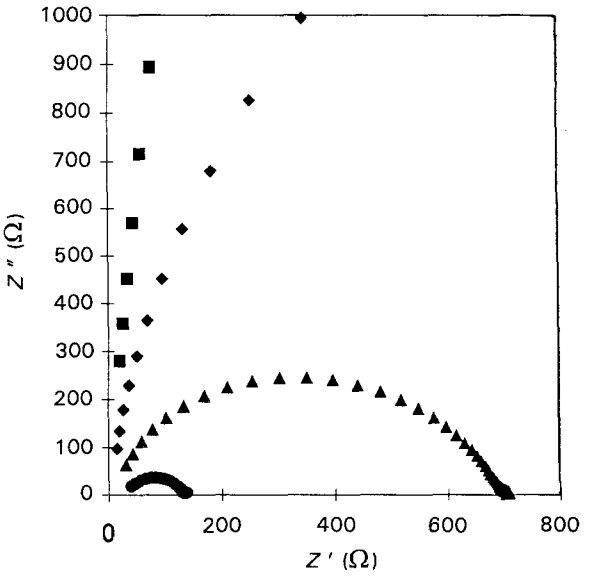

Figure 3 Cole–Cole diagrams for ZBSCMCr with 0.5 Cr_2O_3 mol % at different temperatures: (■) 230 °C, (◆) 330 °C, (▲) 440 °C, (●) 560 °C.

system with 0.5 mol% Cr_2O_3 as a function of temperature. The semicircle observed is associated with grain-boundary electric properties. Otherwise, the semicircle characteristics of the grain electrical properties do not appear in these plots because the electrical resistance is smaller than the grain-boundary resistance. Consequently, the time constant of the electronic transport in the grain will be lower than that associated with the grain-boundary region. Then, the semicircle related to the grain would be characterized only at higher frequencies or higher current densities than that used in this work. Levison and Phillip [21] observed this effect using frequencies up to 100 MHz.

It was observed in Fig. 3 that there was a significant effect of temperature on the Cole–Cole diagram. Therefore in this paper, the impedance data for several temperatures are presented in the Bode diagram form, as shown in Fig. 4. Fig. 5 shows the effect of different Cr_2O_3 additions to the ZBSCMCr system.

Using the transfer function in Fig. 2, we obtain the grain-boundary resistance, R_{GB}; grain resistance, R_G,

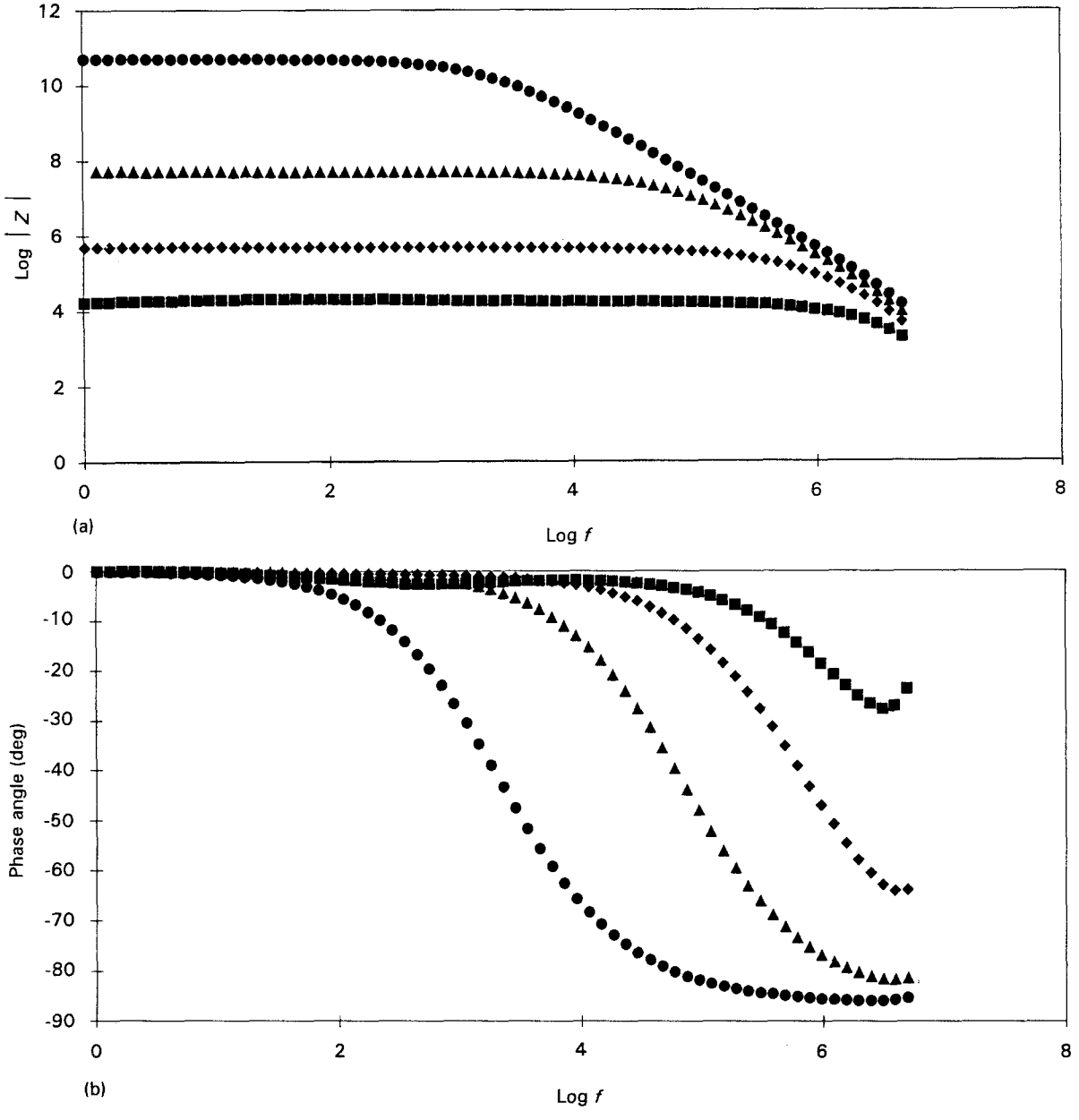

Figure 4 (a, b) Bode diagrams for ZBSCMCr with 0.5 Cr_2O_3 mol % at different temperatures: (●) 230 °C, (▲) 330 °C, (◆) 440 °C, (■) 560 °C.

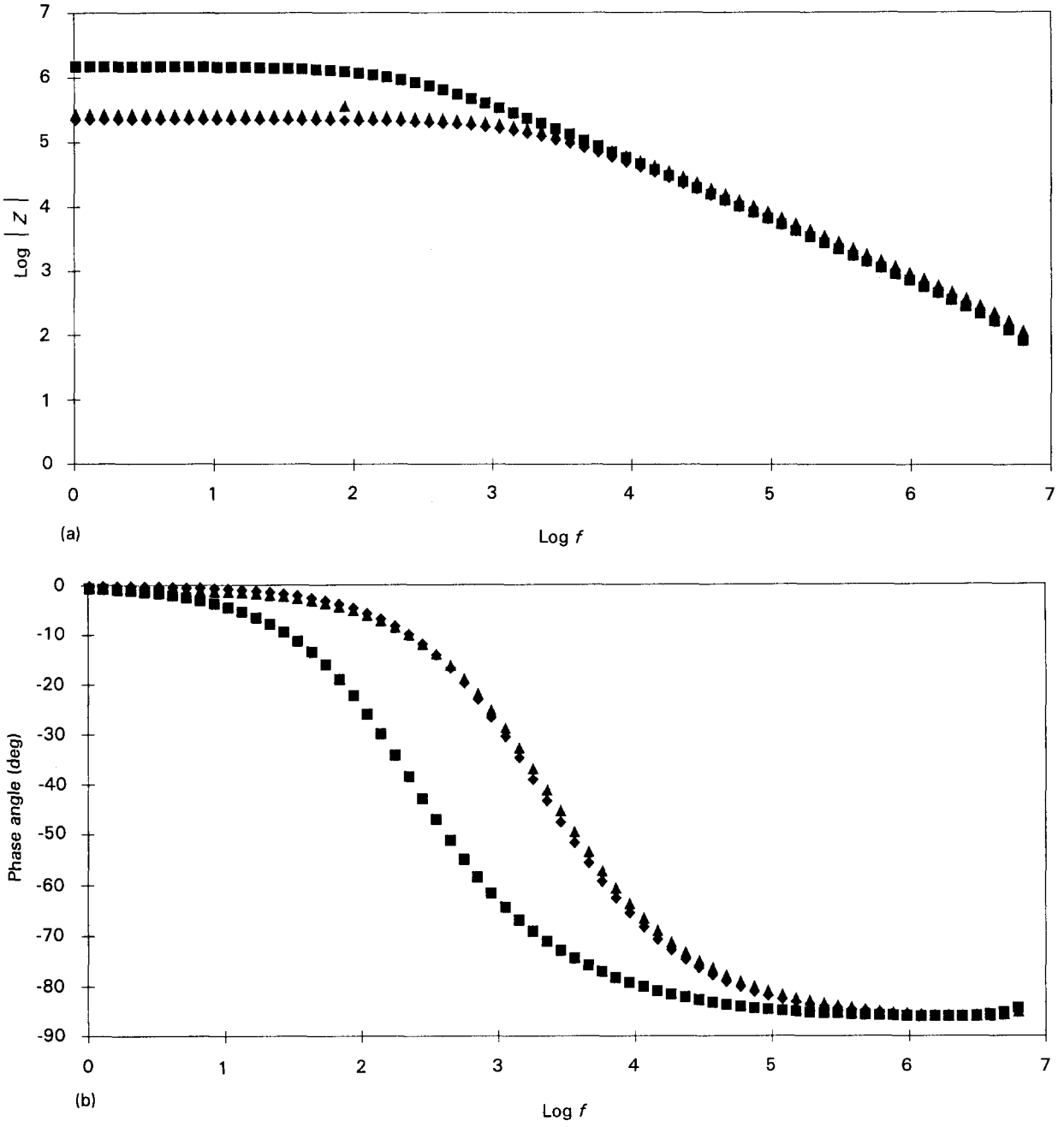

Figure 5 (a, b) Bode diagrams for ZBSCMCr at 330 °C at different Cr_2O_3 concentrations (mol %): (■) 0.1%, (◆) 0.5%, (▲) 0.8%.

and the grain-boundary capacitance, C_{GB}, using the relations

$$\log_{f\to 0}|Z| = \log(R_{GC} + R_G) \quad (1)$$

$$\log_{f\to\infty}|Z| = \log R_G \quad (2)$$

$$C_{GB} = \frac{1}{R_{GB}\omega} \text{ for } \tan(\theta) = 45° \quad (3)$$

where $\omega = 2\pi f$.

Table II presents the parameters calculated from the Equations 1–3 for the different samples. As can be observed, the grain resistance does not change in the experimental error range. This fact indicates that Cr_2O_3 addition does not alter the grain properties. Otherwise, the grain-boundary resistance changes several orders with the addition of Cr_2O_3 from

TABLE II Electric parameters calculated for ZBSCMCr sintered at 1250 °C with different Cr_2O_3 concentrations

Cr_2O_3 (mol %)	T (°C)	R_G (Ω cm)	R_{GB} (Ω cm)	C_{GB} (f cm^{-2})
0.1	230	20.5	5142 514	6.76×10^{-9}
	330	23.7	127 498	1.67×10^{-8}
	440	27.6	9 373	2.59×10^{-8}
	560	64.3	953	4.69×10^{-8}
0.5	230	28.5	1075 728	8.29×10^{-9}
	330	35.5	34 608	1.86×10^{-8}
	440	68.3	3 283	4.08×10^{-8}
	560	144.4	509	2.09×10^{-7}
0.8	230	35.0	1065 160	7.78×10^{-9}
	330	42.6	84 324	1.02×10^{-8}
	440	50.4	13 317	2.07×10^{-8}
	560	76.4	2 284	3.78×10^{-8}

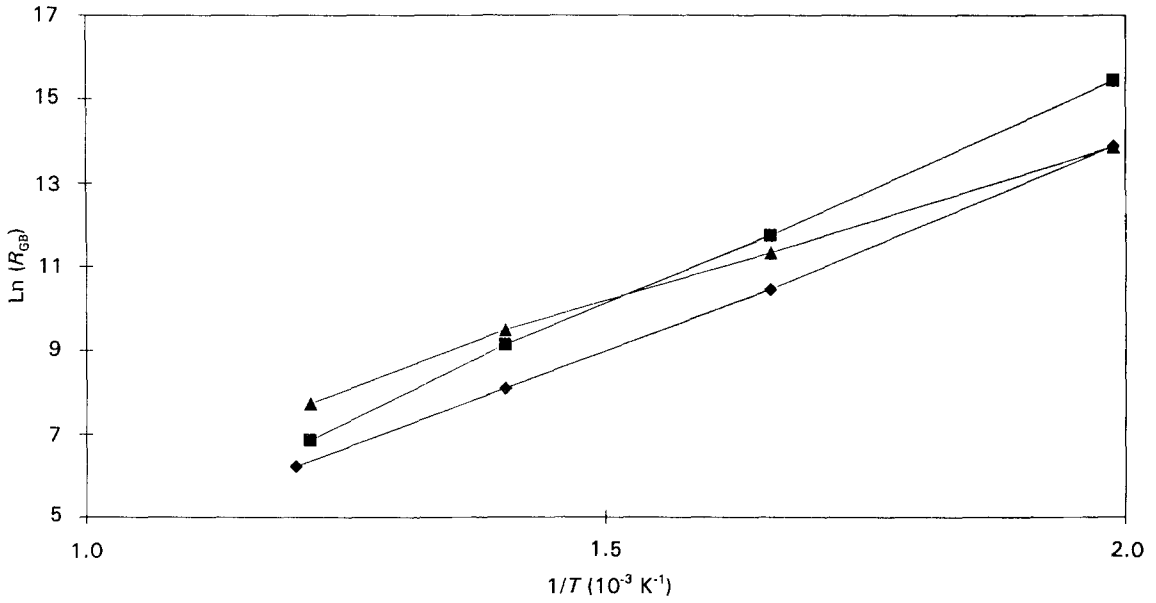

Figure 6 Ln R_{GB} as function of $1/T$ for ZBSCMCr at different Cr_2O_3 concentrations (mol %): (■) 0.1%, (◆) 0.5%, (▲) 0.8%.

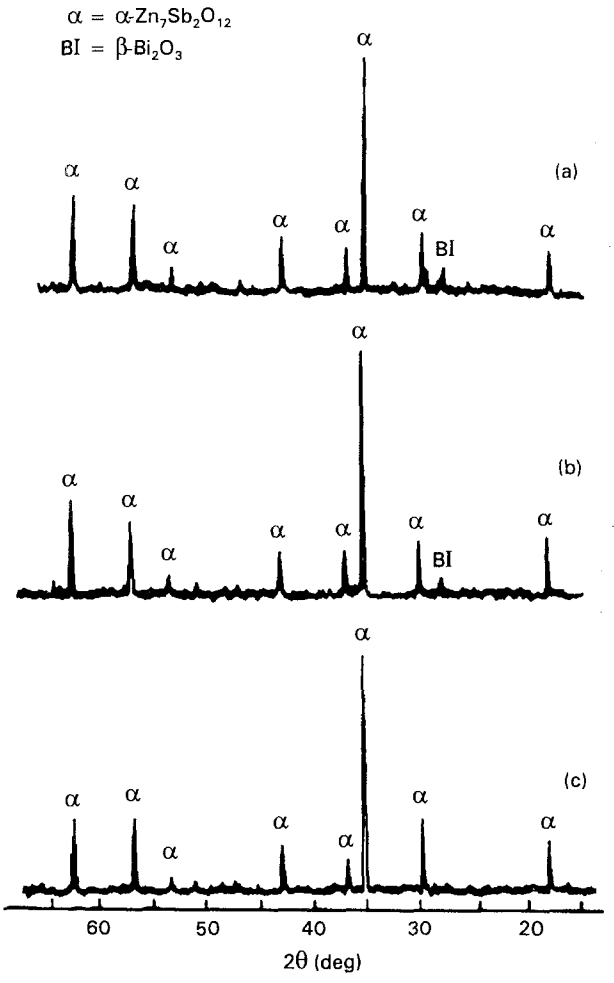

Figure 7 X-ray diffraction patterns for ZBSCMCr with 0.5 Cr_2O_3 sinterized at different temperatures: (a) 1050 °C, (b) 1150 °C, (c) 1250 °C; α = α-$Zn_7Sb_2O_{12}$; BI = β-Bi_2O_3.

0.1–0.8 mol%. The logarithm of the grain resistance as function of the inverse of temperature is illustrated in Fig. 6 and the activation energy for the electronic process at the grain-boundary region is presented in Table III.

TABLE III Energy activation of the electronic process at the grain-boundary region for ZBSCMCr sintered at 1250 °C with different Cr_2O_3 concentrations

Cr_2O_3 (mol %)	ΔE (eV)
0.1	0.95
0.5	0.83
0.8	0.68

The influence of trivalent oxides such as Al_2O_3, Ga_2O_3 on the electrical properties of the ZnO varistors was studied by several authors [22–25]. These oxides are incorporated into the chemical composition of the varistor to lower the electrical resistivity of ZnO grains and to improve the non-linearity in high current densities delaying the onset of voltage upturn. The decrease in electrical resistivity of the ZnO grains is associated with the formation of a substitutional solid solution of these trivalent cations (M^{3+}) by divalent zinc cations (Zn^{2+}) in the ZnO lattice. This solid-state reaction increases the electron concentration in the valence band according to the reaction [22]

$$\tfrac{1}{2}M_2O_3 \xrightarrow{ZnO} M_{Zn}^{\cdot} + e' + Zn_{Zn}^{x} + O_O^{x} + \tfrac{1}{4}O_2(g) \quad (4)$$

In the above equation, the Kröger–Vink notation was adopted [26] where $M_{Zn}^{\cdot}$ denotes a trivalent metal replacing the divalent zinc atoms creating an atomic defect with a effective charge + 1, e′ is a quasi-free electron and Zn_{Zn}^{x}, O_O^{x} are the cation and oxygen ions in their normal lattice position, respectively. Despite the fact that Al_2O_3 and Ga_2O_3 improve the non-linear characteristics of the varistors in high current densities, they exert a detrimental influence on the non-linearity in the low current densities (pre-breakdown region) that is controlled by grain-boundary properties. Literature data show also that these trivalent oxides can be dissolved by the spinel phase [22, 27] or

segregate at the grain boundaries [23]. The presence of Al_2O_3 in the spinel phase does not affect directly the potential barrier at the grain boundaries, but its segregation can decrease the height of the barrier in the pre-breakdown region. Kim and Kim [17] investigated the effect of Co_2O_3 additions to the ZnO varistor at high current densities. It was shown that the upturn region occurs at lower current densities by increasing the Co_2O_3 content. The onset of voltage upturn in CoO-doped varistor is higher than that in the Co_2O_3-doped one at the same cobalt concentration. These effects were explained by the decomposition of the Co_2O_3 into CoO which produces a higher oxygen partial pressure and lowers the conductivity of ZnO grains due to a decrease in donor concentration.

It was observed that the influence of Cr_2O_3 on the electrical properties of a ZnO varistor is different from that for Al_2O_3, Ga_2O_3 and Co_2O_3 dopants. The first consideration is that chromium oxide does not form an extensive solid solution with the ZnO [7, 8] as occurs with those oxides [22]. The second is that the Cr_2O_3 is thermally stable in the range of temperature studied [28] and does not suffer decomposition like Co_2O_3 at high temperatures. Two possibilities can be considered to explain the behaviour of the grain and the grain-boundary resistance with Cr_2O_3 addition shown in Table II: (a) the occurrence of small amounts of a secondary phase with the Cr_2O_3 excess that increase the conductivity of the grain boundary, or (b) small amounts of Cr^{3+} ions segregate at the grain boundaries substituting the Zn^{2+} ions and increasing the electronic density at the ZnO–ZnO interface. Fig. 7 shows the X-ray diffraction patterns for the varistors sintered at different temperatures with 0.5 mol% Cr_2O_3. The ZnO peaks do not appear because ZnO was dissolved by the perchloric acid, as previously described. In addition to the ZnO phase, α-spinel (α-$Zn_7Sb_2O_{12}$) and a bismuth-rich (β-Bi_2O_3) phase were identified. Fig. 8 shows the microstructure of the undoped ($x = 0$) and Cr_2O_3-doped ($x = 0.5$) system. Microanalysis was realized in regions corresponding to secondary phases. The Cr_2O_3 influence on the varistor microstructure is well evinced by the formation of precipitates smaller than that of the undoped system and with a homogeneous distribution. These precipitates are localized at the grain boundaries or in the ZnO grains and correspond to the α-spinel phase. Microanalysis showed that great amounts of Cr_2O_3 and minor amounts of MnO_2 and CoO are dissolved in the spinel phase. The majority of the ZnO grains lacked any continuous intergranular bismuth-rich phase. In order to verify the formation of other phases relative to the Cr_2O_3, we prepared the composition 96.5% ZnO + 1.5% Sb_2O_3 + 2.0% Cr_2O_3 (mol %) and sinterized it at 1050 °C. The X-ray diffraction pattern of this system is shown in Fig. 9 where the ZnO phase was partially dissolved by a dilute solution of $HClO_4$. It was verified that despite the high Cr_2O_3 concentration, only the ZnO and α-$Zn_7Sb_2O_{12}$ phases were identified. Otherwise, for

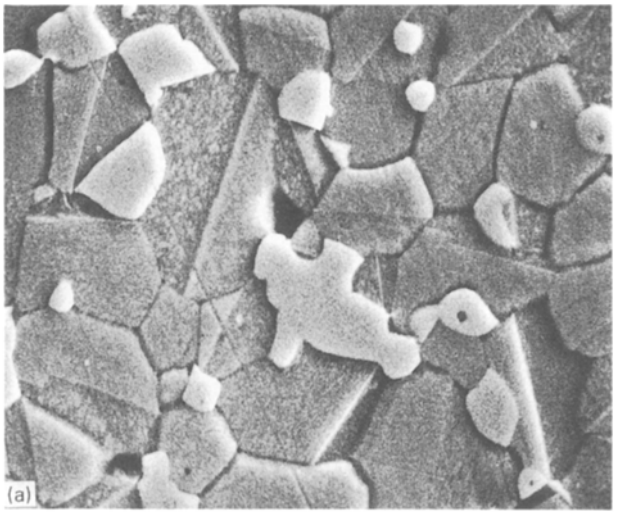

Figure 8 Scanning electron micrographs and microanalysis of the (a, b) undoped and (c, d) doped Cr_2O_3 ZnO varistors. × 3000

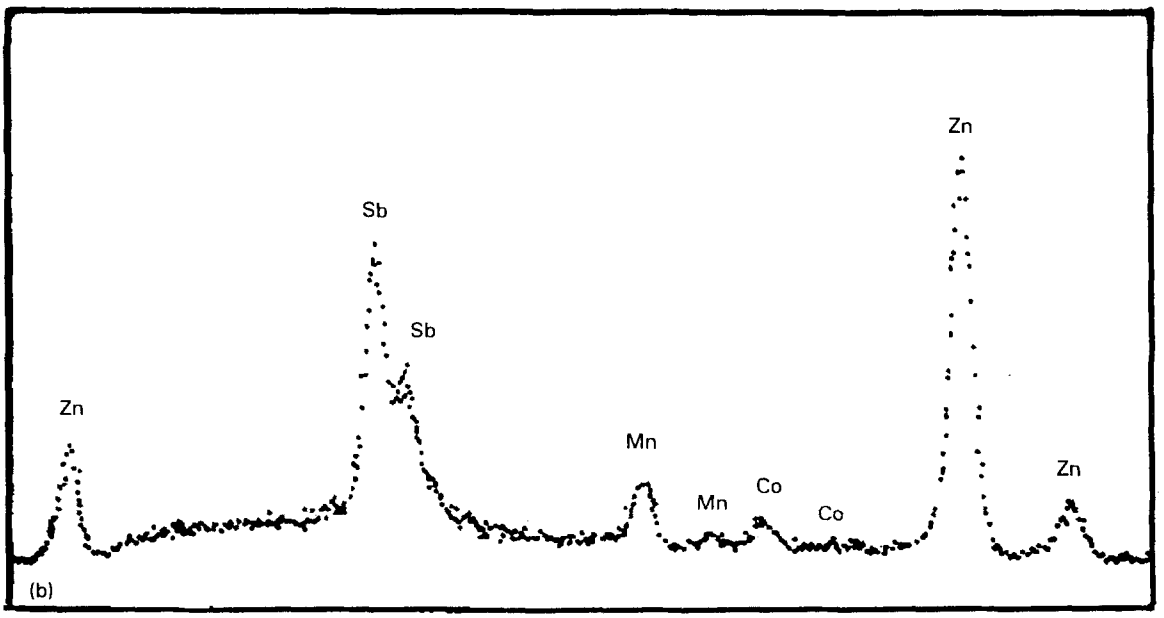

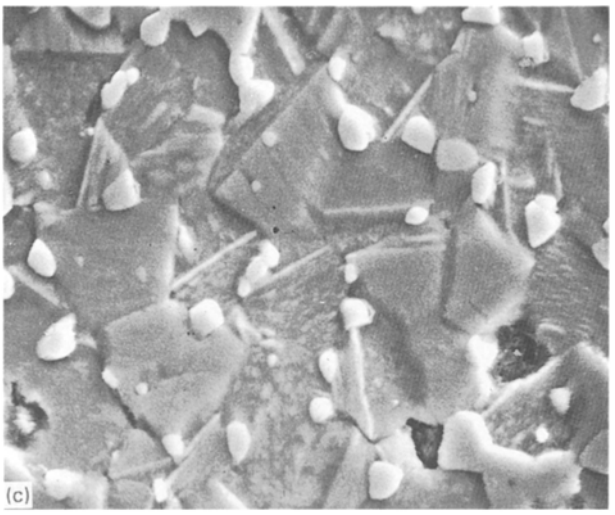

Figure 8 (continued).

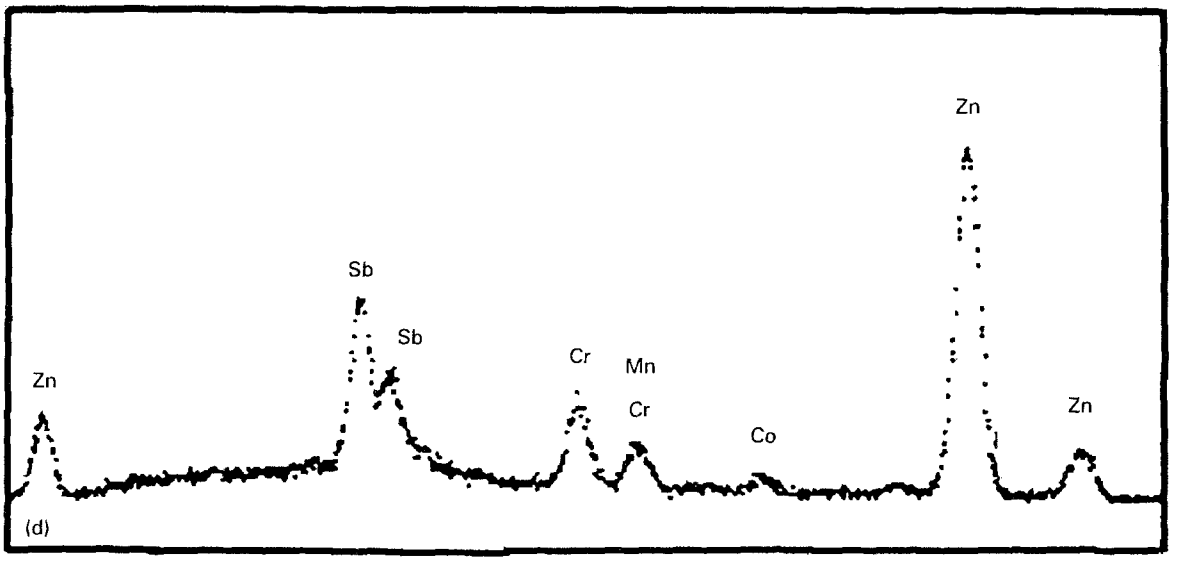

the system 99.0% ZnO + 0.5% Bi_2O_3 + 0.5% Cr_2O_3 the spinel phase $ZnCr_2O_4$ is largely formed, as shown in Fig. 10a. When 1.5 mol% Sb_2O_3 is added to this system, the α-spinel ($Zn_7Sb_2O_{12}$) is preferentially formed and the Cr_2O_3 is dissolved in this phase, as can be seen in the Fig. 10b. In addition to the α-spinel and β-Bi_2O_3, the pyrochlore phase ($Zn_2Bi_3Sb_3O_{14}$) was identified; this decomposes completely in α-spinel and bismuth-rich phases at higher temperatures [7]. Quantitative studies [8] assume that five-sixths of the

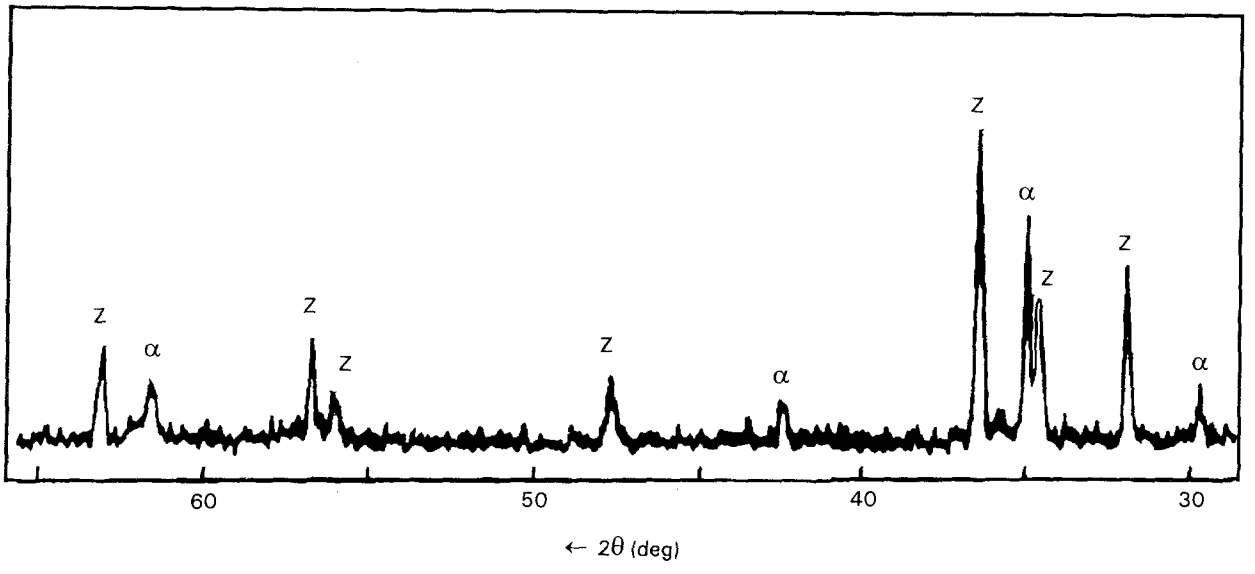

Figure 9 X-ray diffraction patterns for the 96.5% ZnO + 1.5% Sb_2O_3 + 2.0% Cr_2O_3 (mol %) system. Z = ZnO; α = α-$Zn_7Sb_2O_{12}$.

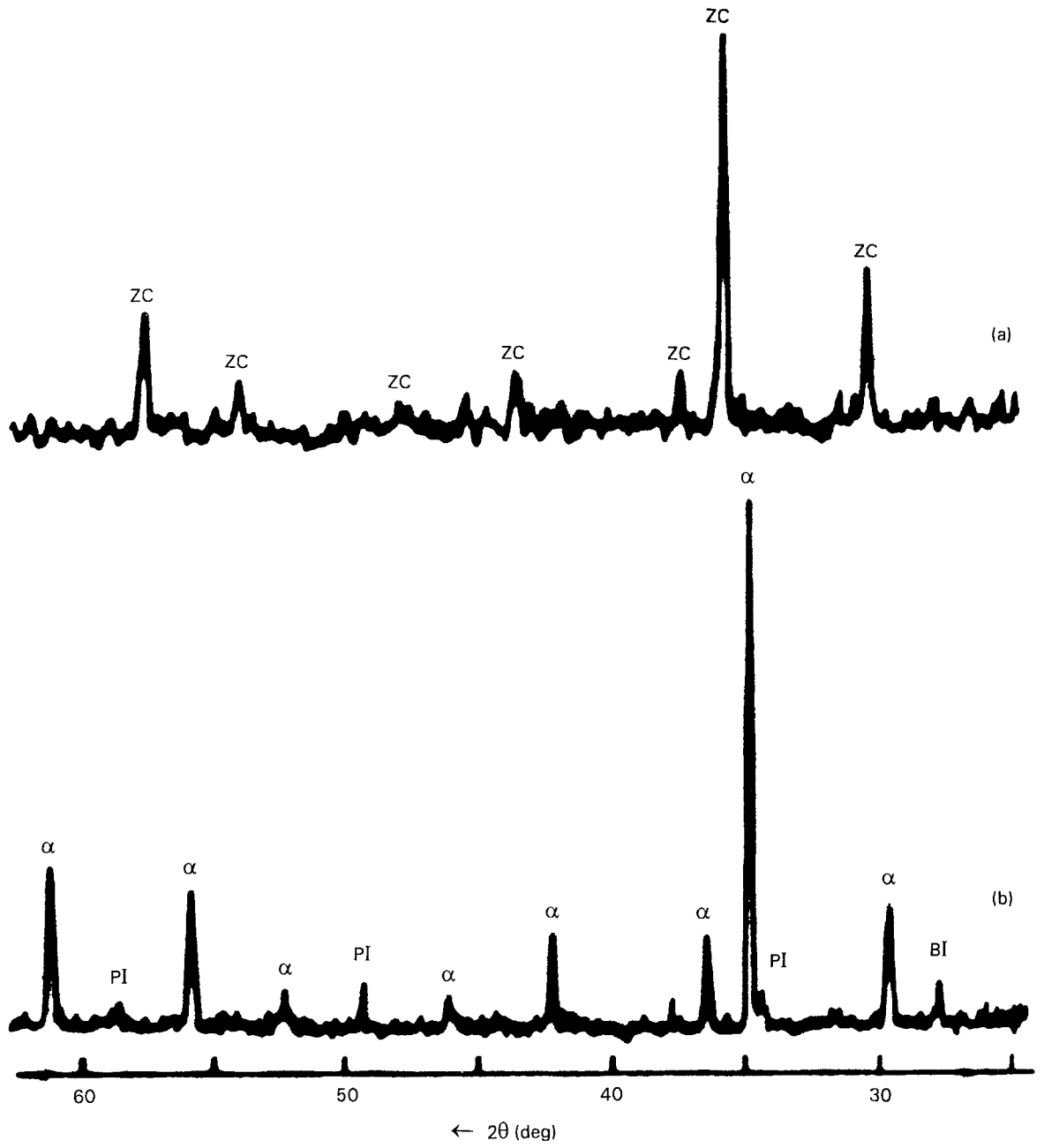

Figure 10 X-ray diffraction patterns for (a) 99.0% ZnO + 0.5% Bi_2O_3 + 0.5% Cr_2O_3 (mol %) system, and (b) 97.5% ZnO + 0.5% Bi_2O_3 + 1.5% Sb_2O_3 + 0.5 % Cr_2O_3 (mol %). Sintering temperature, 1050 °C. α = α-$Zn_7Sb_2O_{12}$; BI = β-Bi_2O_3; PI = $Zn_2Bi_3Sb_3O_{14}$; ZC = $ZnCr_2O_4$.

Cr_2O_3 added goes into the spinel phase and the rest into the bismuth-rich phases. Inada [7] showed that the β-Bi_2O_3 does not dissolve Cr_2O_3. Thus, we assume that the Cr_2O_3 is not dissolved by the spinel phase but is segregated at the grain boundary. This assumption explains the results of current–voltage characteristics of the impedance data. As a consequence of Cr_2O_3 segregation in the interfacial region, the grain-boundary potential barrier height decreases. Then, a reaction can be proposed to explain the influence of the excess Cr_2O_3 on the varistor properties

$$\tfrac{1}{2}Cr_2O_{3\,excess} \xrightarrow{Zn_{GB}} Cr^{\bullet}_{Zn_{GB}} + e' + \tfrac{3}{2}O_2 \qquad (5)$$

where $(Cr_2O_3)_{excess}$ denotes the chromium oxide that is not dissolved in the spinel phase or in the bismuth-rich phase, ZN_{GB} the component stable on the double Schottky barrier [13], $Cr^{\bullet}_{Zn}$ the atomic defect formed with an effective charge + 1, and e′ the quasi-free electron. Thus, the rise in the electron concentration in the conduction band is the main reason for the conductivity increase at the pre-breakdown region.

4. Conclusion

The Cr_2O_3 addition does not change the ZnO grain resistance of a ZnO-based varistor. However, large amounts of Cr_2O_3 addition to a ZnO varistor lower the height of the potential barrier at grain boundaries, increasing the leakage current and decreasing the α value. It is assumed that excess Cr^{3+} not dissolved by spinel or bismuth-rich phase, can segregate at the grain boundary. Then the grain-boundary electrical

resistance decreases, as observed in the pre-breakdown region. The electric field–current density results are corroborated by the activation energy for the grain-boundary process obtained by the impedance experiments.

References

1. M. MATSUOKA, *Jpn J. Appl. Phys.* **10** (1971) 736.
2. J. J. LEE and M. S. COOPER, *IEEE Trans. Parts Hybrids Packaging*, **PHP-13** (1977) 413.
3. J. D. HARNDEN Jr and F. D. MARTZLOFF, *Electron.* **9** (1972) 91.
4. L. M. LEVINSON and H. R. PHILIPP, *IEEE Trans. Parts Hybrids Packaging* **PHP-13** (1977) 338.
5. W. D. NIEBUHR, *IEEE Trans. Ind. Applic.* **IA-21** (1985) 1081.
6. J. E. HARDER, *IEEE Trans. Power Apparatus Systems* **PAS-104** (1985) 2446.
7. M. INADA, *Jpn J. Appl. Phys.* **19** (1980) 409.
8. A. T. SANTHANAM, T. K. GUPTA and W. G. CARLSON, *J. Appl. Phys.* **50** (1979) 852.
9. J. WONG, *ibid.* **46** (1975) 1653.
10. W. D. KINGERY, J. V. D. SANDE and T. MITAMURA, *J. Am. Ceram. Soc.* **62** (1979) 221.
11. H. KANAY, M. IMAY and T. TAKAHASHI, *J. Mater. Sci.* **20** (1985) 3957.
12. L. M. LEVINSON and H. R. PHILIPP, *J. Appl. Phys.* **47** (1976) 1117.
13. T. K. GUPTA and W. G. CARLSON, *J. Mater. Sci.* **20** (1985) 3487.
14. P. L. HOWER and T. K. GUPTA, *J. Appl. Phys.* **50** (1979) 4847.
15. E. R. LEITE, J. A. VARELA and E. LONGO, *J. Mater. Sci.* **27** (1992) 5325.
16. A. MIRALLES, A. CORNET, A. HERMS and J. R. MORANTE, *Mater. Sci. Eng.* **A109** (1989) 201.
17. E. D. KIM and C. H. KIM, *J. Appl. Phys.* **58** (1985) 3231.
18. P. KOSTIC, O. MILOŠVIC and D. USKOKOVIC, *Silic. Ind.* **3–4** (1985) 47.
19. G. E. PIKE, S. R. KURTZ and P. L. GOURLEY, *J. Appl. Phys.* **57** (1985) 5512.
20. K. EDA, *ibid.* **49** (1978) 2964.
21. L. M. LEVINSON and H. R. PHILIPP, *ibid.* **47** (1976) 3116.
22. W. G. CARLSON and T. K. GUPTA, *ibid.* **53** (1982) 5746.
23. H. SHOUXIANG, W. SHILIANG, X. YUCHUN and L. XINGJIAO, *IEEE Trans. Comp. Hybrids Manuf. Technol.* **CMT-8** (1985) 525.
24. T. MIYOSHI, K. MAEDA, K. TAKAHASHI and T. YAMAZAKI, "Advances in Ceramics", Vol. 1, edited by L. M. Levinson (American Ceramic Society, Columbus, OH, 1981) p. 309.
25. H. OKUMA, N. AMIJI, M. SUZUKI and Y. TANNO, "Advances in Ceramics", Vol. 7, edited by M. F. Yan and A. H. Heuer (American Ceramic Society, Columbus, OH, 1983) p. 41.
26. F. A. KRÖGER and H. VINK, "Solid State Physics", edited by F. Seitz and D. Turnbull (Academic Press, New York, 1956) p. 307.
27. T. TAKEMURA and M. KOBAYASHI, "Advances in Ceramics", Vol. 7, edited by M. F. Yan and A. H. Heuer (American Ceramic Society, Columbus, OH, 1983) p. 50.
28. G. V. SAMSONNOV, "The oxide handbook" (IFI/Plenum, New York, 1973) p. 213.

Received 13 October 1993
and accepted 15 June 1994